

Supporting Information for
Enhanced Scale Inhibition against $\text{Ca}_3(\text{PO}_4)_2$ and Fe_2O_3 in
Water Using Multi-Functional Fluorescent-Tagged Antibacterial
Scale Inhibitors

Shaopeng ZHANG ^{a, #}, Xin JIANG ^{a, #}, Shikun Cheng ^b, Chang'e FU ^c, Ziqi TIAN ^d,
Zhen YANG ^{a,*}, Weiben YANG ^{a,*}

^a School of Chemistry and Materials Science, Jiangsu Provincial Key Laboratory of Materials Cycling and Pollution Control, Nanjing Normal University, Nanjing 210023, P. R. China

^b School of Energy and Environmental Engineering, Beijing Key Laboratory of Resource-Oriented Treatment of Industrial Pollutants, University of Science and Technology Beijing, Beijing 100083, P. R. China

^c College of the Environment and Ecology, Jiangsu Open University, Nanjing 210036, P. R. China

^d Ningbo Institute of Materials Technology & Engineering, Chinese Academy of Sciences, Ningbo 315000, P. R. China

[#] Both authors contributed equally.

^{*} Corresponding authors.

E-mail: yangzhen@njnu.edu.cn (Z. Y.), yangwb007@njnu.edu.cn (W. Y.)

Summary

Total pages: 15 (S1-S15)

Text S1. Synthetic method of FM-AA-APEO. (S3)

Text S2. Calculation methods of X and Y in AA-APEO- X and FM-AA-APEO- Y . (S4)

Text S3. Methodologies and results of structural characterization of scale inhibitors. (S5)

Table S1. Coded levels for two variables of fluorescent intensity response in binary-solute solutions containing FM-AA-APEO and calcium ions in RSM analysis. (S6)

Table S2. Coded levels for two variables of fluorescent intensity response in binary-solute solutions containing FM-AA-APEO and ferric ions in RSM analysis. (S7)

Table S3. RSM experimental design and results for fluorescent intensity response in binary-solute solutions containing FM-AA-APEO and calcium ions. (S8)

Table S4. RSM experimental design and results for fluorescent intensity response in binary-solute solutions containing FM-AA-APEO and ferric ions. (S9)

Fig. S1. Synthetic route of scale inhibitor FM-AA-APEO. (S10)

Fig. S2. (a) FTIR, (b) ^1H NMR, (c) UV-vis spectra and (d) TG curves of different samples. (S11)

Fig. S3. Chemical structure of two commercial scale inhibitors (PAPEMP and JH-907). (S12)

Fig. S4. Comparison between experimental and predicted values from RSM regression equations. (S13)

Fig. S5. UV spectra of AA-APEO-1.56% solution with the coexistence of different concentrations of (a) Ca^{2+} and (b) Fe^{3+} . (S14)

Fig. S6. O1s XPS spectra of (a and b) $\text{Ca}_3(\text{PO}_4)_2$ and (c and d) Fe_2O_3 precipitates (a and c) without and (b and d) with the coexistence of FM-AA-APEO. (S15)

Text S1. Synthetic method of FM-AA-APEO.

After certain amounts of AA, APEO and FM (degree of polymerization: 10) with designed ratios was dissolved in 90 mL of water, the solution was kept at 70 °C under magnetic stirring and nitrogen condition for 30 min. Subsequently, initiator solution (0.3 g of ammonium persulfate dissolved in 15 mL of water) was added dropwise over a period of 1 h. The reaction mixture was heated to 80 °C and maintained at this temperature for a further 2 h. Solid scale inhibitor product was finally obtained after precipitation using excessive acetone, washing with ethanol, and vacuum drying at 45 °C for 24 h.

Text S2. Calculation methods of X and Y in AA-APEO- X and FM-AA-APEO- Y .

(1) For 1 mol of APEO repeated unit in AA-APEO- X , there were X mol of AA repeated units. Hence, mass of C and H atoms could be expressed as follows:

$$M_{(C \text{ atoms})} = (3X+23) \text{ mol} \times 12 \text{ g/mol} = (36X+276) \text{ g};$$

$$M_{(H \text{ atoms})} = (4X+46) \text{ mol} \times 1 \text{ g/mol} = (4X+46) \text{ g}.$$

Therefore, $M_{(C \text{ atoms})}/M_{(H \text{ atoms})}$ equaled $(36X+276)/(4X+46)$, where the mass ratio of C and H was obtained from elemental analysis.

(2) Performance results of AA-APEO in Section 3.1 showed that the optimized molar ratio of AA:APEO was 8:1 in AA-APEO. Thus, the ratio of AA:APEO of 8:1 was further used in the trinary copolymers (FM-AA-APEO). For Y mol of FM repeated unit in FM-AA-APEO- Y , there were $[8 \times (1-Y)/9]$ mol of AA and $(1-Y)/9$ mol of APEO units, respectively. Hence, mass of C and N atoms can be expressed as follows:

$$M_{(C \text{ atoms})} = [3 \times 8 \times (1-Y)/9 + 23 \times (1-Y)/9 + 22Y] \times 12 \text{ g/mol} = (188 + 604Y)/3 \text{ g};$$

$$M_{(N \text{ atoms})} = 3 \times Y \text{ mol} \times 14 \text{ g/mol} = 42Y \text{ g};$$

Therefore, $M_{(N \text{ atoms})}/M_{(C \text{ atoms})}$ equaled $63Y/(94 + 302Y)$, where the mass ratio of N and C is obtained from elemental analysis.

Text S3. Methodologies and results of structural characterization of scale inhibitors.

FTIR spectra were recorded on a Bruker Tensor 27 IR spectrometer system using samples pelletized with KBr. ¹H NMR spectra were recorded on a Bruker model AVANCE400 NMR spectrometer using D₂O as the solvent. UV-vis spectra were recorded on a Hitachi UH-5300 UV-vis spectrophotometer. Elemental analysis was conducted on a Vario EL III elemental analyzer. Thermogravimetric (TG) analysis was performed on a Diamond DMA spectrometer.

The FTIR spectra were shown in SI Figure S2a. Peaks at 1730 and 1107 cm⁻¹ indicated C=O and C-O in FP-AA-APEO, respectively. Besides, characteristic peaks of FM monomers at 787 and 1398 cm⁻¹ (C-N in N-methyl piperazine) remained slight peaks in the final FM-AA-APEO. ¹H NMR spectra in SI Figure S2b confirmed that the main structure of the designed inhibitor FM-AA-APEO was found. UV spectra in SI Figure S2c demonstrated that, the final FM-AA-APEO owned the main adsorption peak at 388 nm due to the existence of FM groups, while AA-APEO08 did not. TG curves in SI Figure S4d showed that, FM-AA-APEO-1.56% had better thermal stability than AA-APEO-8 without the fluorescent groups.

Table S1. Coded levels for two variables of fluorescent intensity response in binary-solute solutions containing FM-AA-APEO and calcium ions in RSM analysis.

Factors	Range and Levels				
	-2	-1	0	1	2
X ₁ : Ca ²⁺ (mg/L)	200	400	600	800	1000
X ₂ : Dosage (mg/L)	2	4	6	8	10

Table S2. Coded levels for two variables of fluorescent intensity response in binary-solute solutions containing FM-AA-APEO and ferric ions in RSM analysis.

Factors	Range and Levels				
	-2	-1	0	1	2
X ₁ : Fe ³⁺ (mg/L)	5	10	15	20	25
X ₂ : Dosage (mg/L)	2	10	18	26	34

Table S3. RSM experimental design and results for fluorescent intensity response in binary-solute solutions containing FM-AA-APEO and calcium ions.

	Ca²⁺ concentration ^a	Dosage ^a	Experimental value	Predicted value
1	2 (1000)	-2 (2)	138.6	158.44
2	-2 (200)	2 (10)	1310	1294.16
3	-1 (400)	0 (6)	731.9	747.73
4	1 (800)	1 (8)	962.6	958.09
5	0 (600)	0 (6)	711.8	726.14
6	0 (600)	1 (8)	978.7	988.56
7	2 (1000)	0 (6)	668.0	656.2
8	0 (600)	-2 (2)	232.9	228.54
9	1 (800)	-1 (4)	465.1	442.25
10	1 (800)	0 (6)	688.3	695.63
11	0 (600)	2 (10)	1247	1260.06
12	0 (600)	-1 (4)	484.2	472.8
13	-2 (200)	-2 (2)	260.7	262.96
14	-1 (400)	1 (8)	1020	1010.11
15	2 (1000)	2 (10)	1192	1190.28
16	-1 (400)	-1 (4)	509.1	494.43
17	-2 (200)	0 (6)	746.1	760.4

^a Values outside and inside brackets are encoded and actual (unit for dosage and Ca²⁺ concentration: mg/L) values, respectively.

Table S4. RSM experimental design and results for fluorescent intensity response in binary-solute solutions containing FM-AA-APEO and ferric ions.

	Fe³⁺ ^a	Dosage ^a	Experimental value	Predicted value
1	-2 (5)	2 (34)	3177.31	3008.88
2	2 (25)	-2 (2)	24.14	198.8
3	0 (15)	-1 (10)	973.30	996.64
4	1 (20)	1 (26)	2335.90	2532.24
5	0 (15)	0 (18)	1889.62	1822.88
6	1 (20)	0 (18)	1851.40	1878.4
7	0 (615)	2 (34)	3016.79	2998.48
8	-2 (5)	0 (18)	1930.96	1779.52
9	-1 (10)	1 (26)	2603.21	2470.64
10	0 (15)	1 (26)	2424.37	2490.16
11	2 (25)	0 (18)	1801.89	1956.48
12	-1 (10)	0 (18)	1920.68	1789.92
13	-2 (5)	-2 (2)	81.07	-85.68
14	1 (20)	-1 (10)	912.30	1065.6
15	2 (25)	2 (34)	2928.48	3078.32
16	-1 (10)	-1 (10)	1033.25	950.24
17	0 (15)	-2 (2)	38.28	11.44

^a Values outside and inside brackets are encoded and actual (unit for Fe²⁺ concentration and dosage: mg/L) values, respectively.

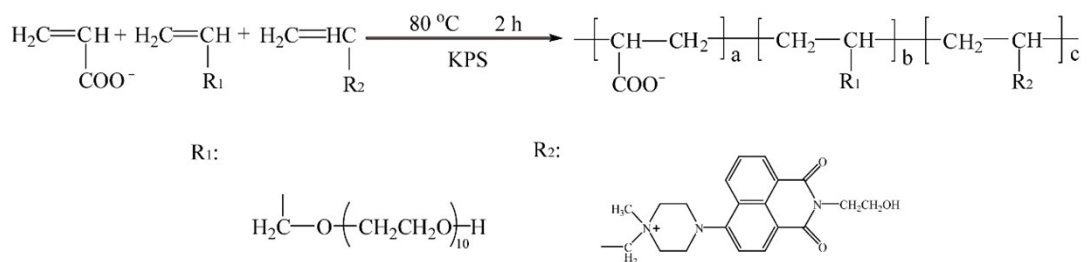
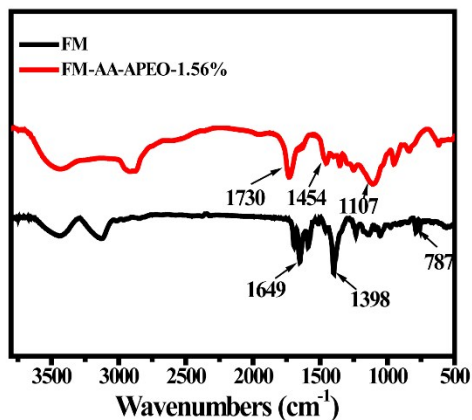
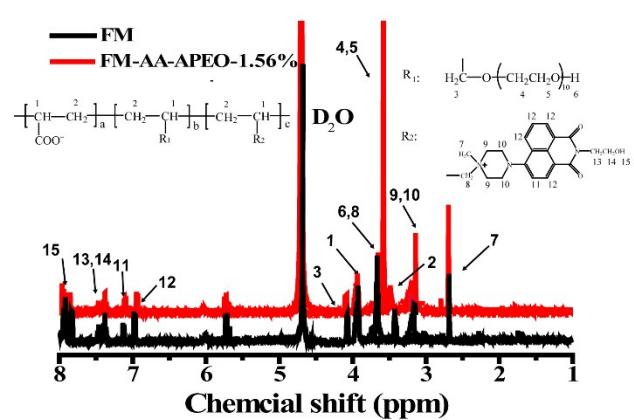


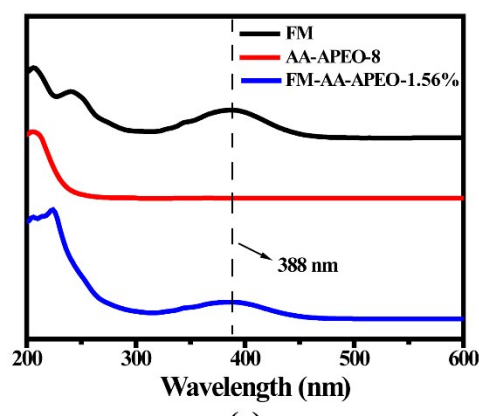
Fig. S1. Synthetic route of scale inhibitor FM-AA-APEO.



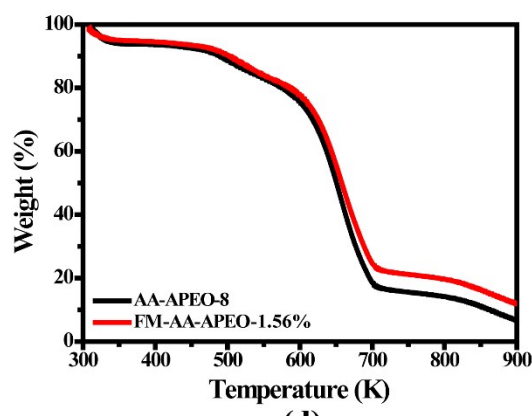
(a)



(b)



(c)



(d)

Fig. S2. (a) FTIR, (b) ^1H NMR, (c) UV-vis spectra and (d) TG curves of different samples.

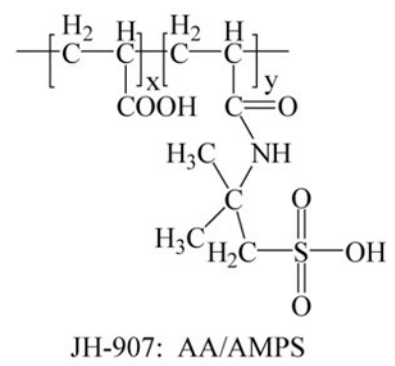
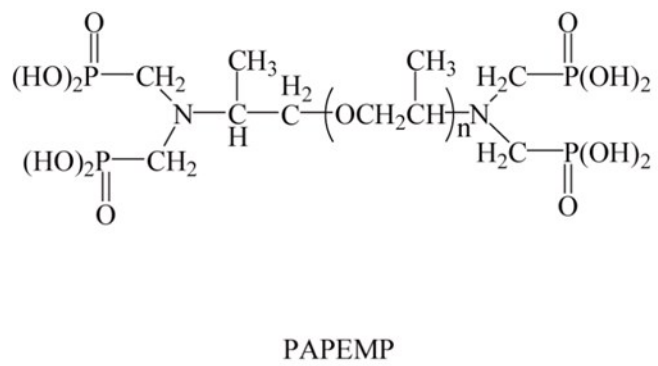


Fig. S3. Chemical structure of two commercial scale inhibitors (PAPEMP and JH-907).

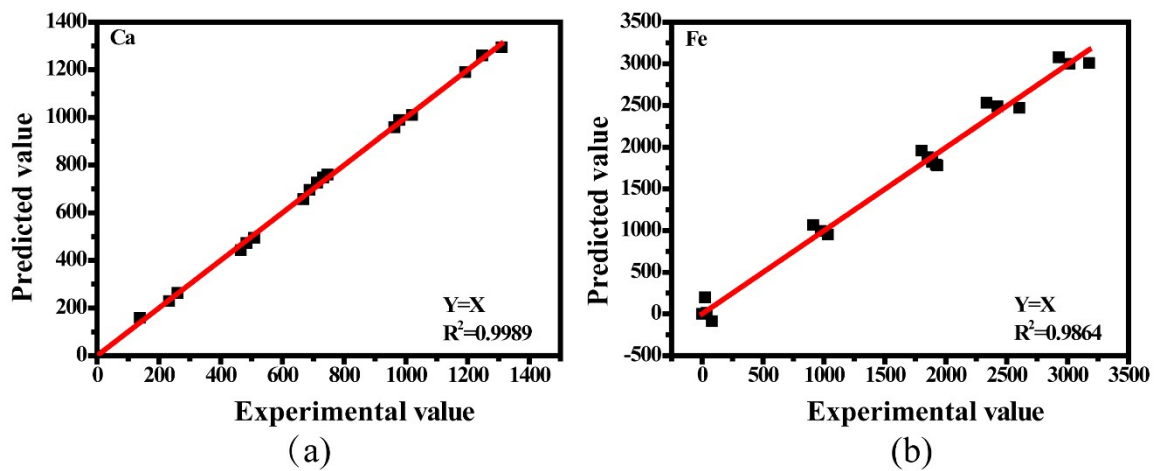


Fig. S4. Comparison between experimental and predicted values from RSM regression equations.

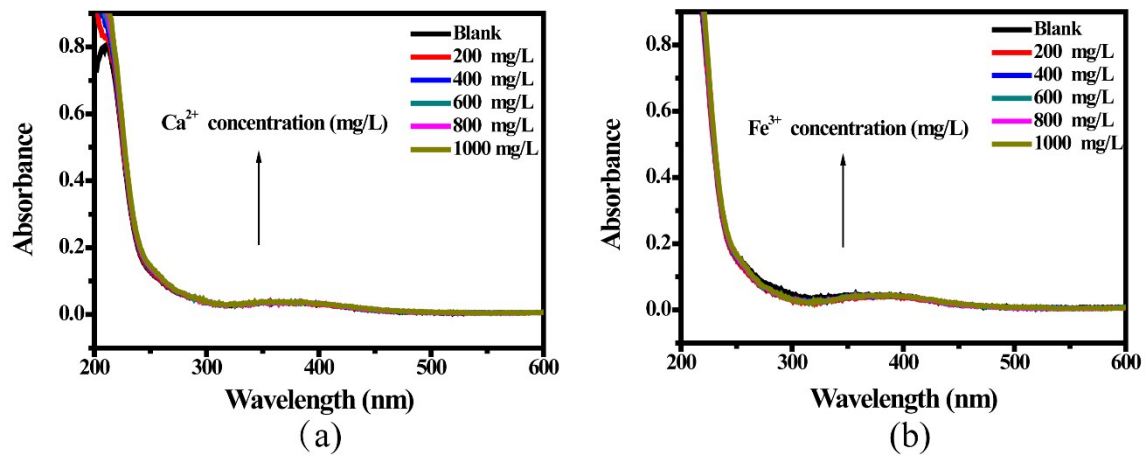


Fig. S5. UV spectra of AA-APEO-1.56% solution with the coexistence of different concentrations of (a) Ca²⁺ and (b) Fe³⁺.

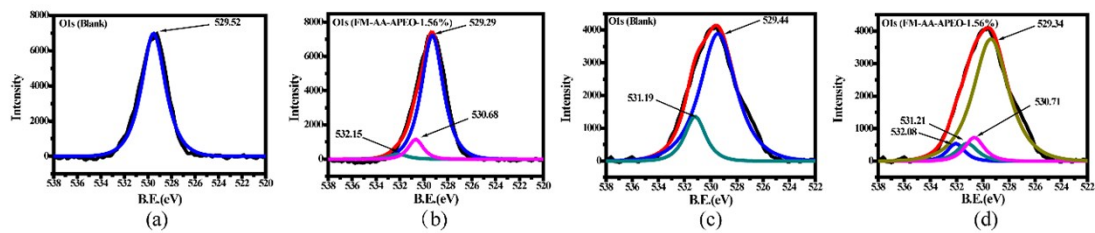


Fig. S6. O1s XPS spectra of (a and b) $\text{Ca}_3(\text{PO}_4)_2$ and (c and d) Fe_2O_3 precipitates (a and c) without and (b and d) with the coexistence of FM-AA-APEO.